Multiscale and Multidisciplinary Modeling, Experiments and Design
https://doi.org/10.1007/s41939-023-00341-y

ORIGINAL PAPER

Hybridization of aluminum–silicon alloy with boron carbide and ferrotitanium: impact on mechanical properties for automotive applications

Oluwafemi Timothy Oladosu[1] · Abayomi Adewale Akinwande[2] · Olanrewaju Seun Adesina[1] · Olufemi Oluseun Sanyaolu[1] · Babatunde Abiodun Obadele[3]

Received: 2 August 2023 / Accepted: 9 December 2023

Abstract
The present study investigated the influence of adding FeTi as supplementary reinforcement to B_4C in an aluminum–silicon (Al-12Si) matrix for automobile applications. The FeTi alloy was introduced at 3, 6, and 9 wt.% alongside 5 wt.% B_4C particles. The effects of such addition on the morphology, physical, and mechanical properties were examined. The X-ray diffraction pattern identified the presence of B_4C and FeTi reinforcing phases alongside Al_3Fe and Ti_5Si_3 phases. The examined morphology revealed that the particles were well dispersed in the matrix, with consequent effects on their properties. Porosity was reported to reduce linearly with rise in FeTi dosage, consequently resulting in a linear increase in density and relatively high overall density. Inclusive of the hardness, the yield and ultimate strength were enhanced progressively upon a progressive rise in FeTi dosage, with a contrary reduction in ductility. The result revealed that the inclusion of FeTi reinforcing fillers in the matrix is capable of ensuing appreciable improvement in the mechanical properties of the composite.

Keywords Aluminum matrix composite · Ferrotitanium · FeTi · Auto-material · Boron carbide · Powder metallurgy · Fractography · Hybridization

1 Introduction

Global realities such as climate change, environmental sustainability, and material innovation have made the production of eco-efficient materials virtually unavoidable. Fuel consumption in automobiles can be reduced by improving the thermodynamic efficiency of the engine, but considerable improvements can also be by reducing the vehicle's weight (Khademian and Peimaei 2020; Patel et al. 2018). Steels and cast iron are utilized in the automobile (Musfirah and Jaharah 2012); however, when seeking for alternative materials, aluminum alloys, magnesium alloys, and polymer composites are ideal for use in automotive applications (Han et al. 2022; Haber 2015; Joost and Krajewski 2017). When compared to other materials, aluminum and its alloys are seen as the preferable options due to their high strength, ductility, conductivity, and low cost (Akinwande et al. 2023a, b; Adediran et al. 2023; Dursun and Soutis 2014). In this context, the proportion of aluminum alloys in all materials used in the design of automobile component is steadily increasing, which has the positive impact of reducing the total mass of vehicles with the aim of minimizing fuel consumption (Adediran et al. 2021; Sharma et al. 2020; Zheng et al. 2018; Orłowicz et al. 2015).

Recent research events have involved the development of aluminum composites and hybrid aluminum composites to improve the mechanical, tribological, and corrosion performance of monolithic aluminum and its alloys. Various aluminum grades play a pivotal role in advancing composite materials. A356 aluminum–silicon alloy, reinforced with granite and graphite particles, exhibits improved friction resistance (Satyanarayana et al. 2019). Al6061, combined

✉ Oluwafemi Timothy Oladosu
otoladosu@gmail.com

✉ Abayomi Adewale Akinwande
abypublications@gmail.com

[1] Department of Mechanical Engineering, Redeemer's University, Ede, Osun State, Nigeria

[2] Department of Metallurgical and Materials Engineering, Federal University of Technology, Akure, Ondo State, Nigeria

[3] Department of Chemical, Materials and Metallurgical Engineering, Botswana International University of Science and Technology, Palapye, Botswana

Published online: 13 January 2024

with SiC and B4C powders through powder metallurgy, demonstrates optimized mechanical properties, with the highest hardness observed in 12%B4C reinforced composites (Halil et al. 2019). AA7075 alloy, used in pumice-reinforced aluminum syntactic foams, shows the impact of particle size, bimodality, and heat treatment on mechanical properties (Bolat et al. 2021). Sahu et al. (2020) explore the microstructure and compressive behavior of 2014 aluminum cenosphere syntactic foam, emphasizing its high strength and unique deformation characteristics. These studies highlight the versatility of aluminum grades in tailoring composite material properties.

Among a large group of aluminum alloys, aluminum–silicon alloy has gained high patronage for automobile designs due to its high casting potency, strength-to-weight ratio, low thermal expansion, and wear resistance. It has found applications in engine components of land automobiles (Akinwamide et al. 2020; Alshmri 2013). Due to the working conditions of automobile engines, efforts have been made to further improve the performance of aluminum–silicon alloys through particulate reinforcement of the matrix. Ceramic particles are often used in the reinforcement of aluminum alloys, consequently improving strength performance, as realized in studies by Balogun et al. (2022), Kumar et al. (2023a, b), and Ogunsanya et al. (2022, 2023). In these studies, improvements were observed in the employed aluminum matrix owing to the intrinsic brittleness of ceramic reinforcement. However, the incorporation of the reinforcement into the metal matrix has eventually led to a reduction in strength at a certain weight proportion (Olaniran et al. 2022a; Ogunbiyi et al. 2023). More so, the brittle nature of the particles often limits ceramic-reinforced aluminum composites in hot–cold-cryo rolling and extrusion processes (Oloruny-olemi et al. 2022). The reports by Akinwande et al. (2023c) had shown the importance of engaging metal-based particles as a supplementary additive to ceramic reinforcement in an aluminum matrix.

The concept of hybridization in aluminum composites involves combining different types of reinforcement particles to fabricate hybrid materials with enhanced properties. This approach aims to capitalize on the unique advantages offered by various types of reinforcements, such as ceramics, to achieve a synergistic effect in terms of mechanical and tribological characteristics (Akinwamide et al. 2021). For instance, Chandel et al. (2021) underscores the significance of incorporating both soft and hard reinforcement particles to reduce brittleness and enhance wear resistance. The use of ceramics like silicon carbide (SiC), graphite (Gr), aluminum nitride (AlN), alumina (Al2O3), and boron carbide (B4C) are highlighted for their potential to significantly improve mechanical and wear characteristics. The inclusion of agro-waste derivatives further adds to the versatility of hybrid composites. Bolat et al. (2022) extends this concept to ceramic-filled aluminum syntactic foams, exploring the effects of reinforcement diameter on compressive features. The study demonstrates the stability of microstructures with uniform distribution, and artificial aging treatment is found to enhance mechanical properties. Ramadoss et al. (2020) contributes to this concept by synthesizing B4C and BN reinforced Al7075 hybrid composites, showing increased hardness and improved compressive properties. The research explores the interfacial reactions and homogeneous distribution of hybrid reinforcement particles in the base metal matrix.

Recent studies have explored the use of boron carbide (B4C) as a filler in aluminum matrix composites (AMCs) based on its low density, cost-effectiveness, and compatibility with aluminum base materials (Xu et al. 2019). Xu et al. (2019) investigated the impact of B4C particle size on the mechanical properties of aluminum matrix-layered composites, revealing that B4C enhanced impact strength and ultimate tensile strength while lowering composite hardness. Sharma et al. (2019) conducted a comprehensive review of B4C-reinforced AMCs, highlighting the formation of precipitates in B4C-Al interfacial interactions that reduce age-hardening capacity. Increasing B4C percentage and decreasing size improved strength, hardness, and wear resistance up to a certain point, with wear rate influenced by applied weight, sliding duration, and speed. However, limitations such as poor wettability, embrittleness and porosity in AMCs with ceramic reinforcement led to the suggestion of metal-based additives as supplements (Das et al. 2014). In a stir casting approach, Mazahery et al. (2012) aimed to fabricate lightweight Al356 matrix composites with B4C particles, showing improved hardness and tensile strength. Strength significantly improved with 10% of B4C, but further increases led to reduced strength, possibly due to particle agglomeration and increased microporosity.

The inclusion of a metal reinforcement, such as ferrotitanium in this present study, in Al/Si/B4C composites is prompted by challenges associated with ceramic reinforcements like B4C as initially highlighted. To address these limitations, introducing a metal reinforcement offers advantages such as improved ductility, toughness, and enhanced compatibility with the aluminum matrix. Metal additives can mitigate the brittleness of ceramics and foster better interfacial interactions, potentially optimizing the overall mechanical performance of the composite for applications in dynamic and impact-loaded conditions (Olaniran et al. 2023). The major characteristics that make ferrotitanium an appealing material include an outstanding strength–weight ratio, which has led to ferrotitanium being widely used in the aerospace and petrochemical sectors. Yilmaz et al. (2022) conducted a metallographic analysis and studied the wear behavior of Cu-based FeTi-reinforced composites. Cu-based FeTi-reinforced metal matrix composites (MMCs)

were manufactured by powder metallurgy with FeTi reinforcement additions at 6, 9, 12, 15, and 18 wt.%. The interface microstructure between FeTi and Cu at 1000 °C was found to be significantly different, and the hardness altered correspondingly with the increase of FeTi particles. A study on the microstructural and mechanical properties of stir-cast aluminum composite was carried out by Akinwamide et al. (2020), where SiC and FeTi were incorporated into the matrix at varying dosages of 2 and 5 wt.% saw improvement in the mechanical properties. In the same vein, Akinwamide et al. (2019a, b) showed the role of ferrotitanium and silicon carbide on the properties in enhancing the properties of aluminum matrix.

Limitations attached to AMCs are sometimes attributed to the choice of preparation method (Mazahery and Ostad Shabani 2012). Popular methods of producing composites include powder metallurgy and stir casting. However, powder metallurgy has been shown to yield better results compared to other processes like liquid metallurgy based on dimension accuracy, better surface finish, higher strength performance, and better durability (Parikh et al. 2023; Sankhla et al. 2022; Khan et al. 2020). Ferrotitanium has been established to have optimized mechanical properties for various engineering applications. However, studies involving the combination of FeTi and boron carbide in aluminum–silicon alloy are to the best of our knowledge, very rare. This study stands at the forefront of innovation by introducing ferrotitanium as a supplementary reinforcement in Al-12Si/B4C composites using powder metallurgy route. The combination of these elements (FeTi and B4C) aims to overcome the limitations associated with traditional ceramic reinforcements, providing a unique perspective on enhancing the mechanical properties of aluminum alloys. The originality of this work lies in its exploration of the synergistic effects of ferrotitanium alongside lightweight ceramic boron carbide, contributing to a nuanced understanding of the microstructural intricacies. The practical implications of this research extend to potential applications in lightweight automotive components, where improved strength and ductility are paramount. By addressing the challenges posed by ceramic reinforcements, this study offers a fresh perspective on composite materials, aligning with the global pursuit of eco-efficiency and high-performance solutions for various engineering applications.

2 Materials and method

2.1 Materials

The matrix material used for this study is an aluminum–silicon alloy (Al-12Si) with a particle size range of 25–56 μm and a major percentage weight of 86.3% Al and 12.3% Si. The selection of the Al-12Si particle size in this study was chosen based on the research conducted by Sharma et al. (2022).

The image of the scanning electron microscope and elemental composition are indicated in Fig. 1a , b. As received, reinforcing powders are boron carbide and ferrotitanium of average size 12 μm each. The morphology and elemental composition of the powders are shown in Fig. 1c–f.

2.2 Composites fabrication

Powder metallurgy manufacturing process was employed to fabricate the composites. The as-received Al-12Si alloy powder and the as-received B_4C and FeTi powder were mixed homogeneously using a planetary ball mill (ASEW-238). Al-12Si powder was mixed with a constant 5 wt.% B4C and varying amounts of FeTi (3, 6, and 9 wt.%). The ball mill was operated continuously for 6 h at 100 rpm and 25 °C under argon atmospheric conditions. To prevent plastic deformation and overheating of the particle mixes, steel spheres were not used during the mixing operation. A graphite hammer was employed to compress the composite particles for 20 min at a pressure of 45 MPa. The sintering was done in a vacuum microwave sintering furnace (HY-QS1516E) at a 500 °C constant temperature, 25 °C/min heating rate, and a 15-min holding time. The sintered specimens were cut into sections by an electric discharge machining procedure. For reference purposes, the as-received Al-12Si was blended with B_4C and fabricated by subjecting the powder mix to the same fabrication procedure and tagged "reference composite (Al-12Si/5B_4C)."

2.3 Microstructural examination of the composites

To facilitate comprehensive microstructural examination, the specimens underwent a meticulous metallographic preparation process. For this process, the specimen were machined into dimension of 5 × 5 × 5 mm, followed by a systematic polishing regimen involving emery sheets with varying grit sizes (400, 600, 800, 1000, and 1200) and subsequent disk polishing. This stepwise polishing procedure aimed to achieve a pristine surface, accentuating the contrast between the soft and hard matrix of the material. Subsequently, the specimens were mounted with epoxy, providing stability and facilitating handling during subsequent processing. Grinding and polishing ensued until a mirror-like surface was attained, ensuring optimal conditions for microstructural examination. For chemical etching, Kroll's solution, comprising 3 ml hydrofluoric acid (HF) and 5 ml nitric acid (HNO3), was applied to the polished surface for 30 s. Following the etching process, the specimens were thoroughly rinsed with distilled water and dried using a laboratory dryer for one minute.

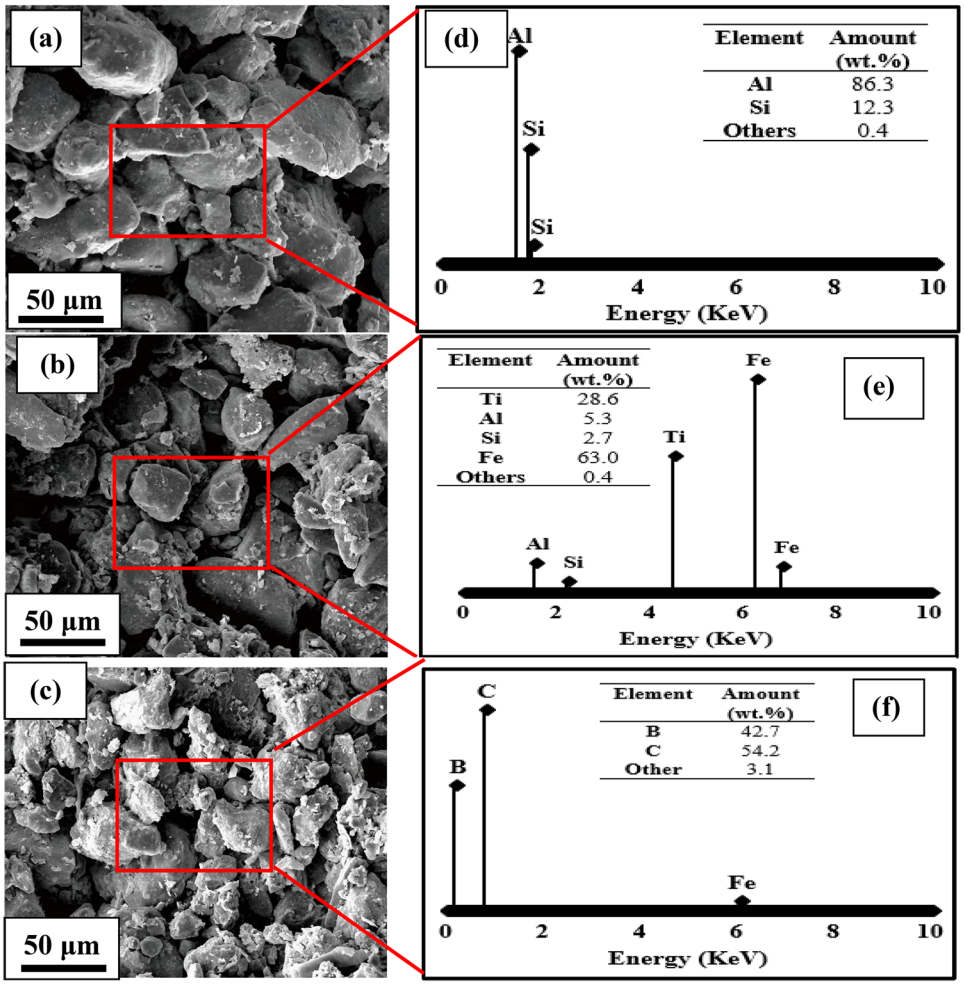

Fig. 1 Microstructure images of **a** aluminum silicon alloy **b** ferrotitanium **c** boron carbide and the chemical composition as analyzed by EDX for **d** aluminum silicon alloy **e** ferrotitanium **f** boron carbide

Afterwards, microstructural analysis was done on the fabricated composites using a scanning electron microscope (JSM-7601F) equipped with an energy dispersive spectrometer attachment (EDS AZ-tec). The SEM was also used to capture the microstructure of the fractured surface of the fractured samples. While the phases present in the composites were determined by an ADX8000 (ANGSTROM) X-ray diffractometer. This was done at 2° angles ranging from 0° to 90°, and the analysis was performed at 40 mA and 45 kV. Further analysis was performed using X'Pert Highscore Plus.

2.4 Assessment of the physical properties

The density of the prepared composites was calculated by the Archimedes' principle, and the determination of the produced composites weight was done with an accuracy of 0.0005 g on an AE200 gauging balance. 10 × 10 × 10 mm specimens were subjected to the test, and six specimens representing each composition were evaluated using this method. The calculation method (expressed in Eq. 1) was employed to determine the theoretical densities of the composites.

$$C_d = [D_m \times (1 - Vr)] + (R \times Vr), \tag{1}$$

where C_d stands for composite density and D_m is matrix density, even as R is the reinforcing powders density. In estimating the relative density (R), measured density (D_m) was divided by the theoretical density (T_d) as showcased in Eq. 2.

$$RD = {}^{D_m}/_{T_d}. \tag{2}$$

Meanwhile, the porosity was estimated via Eq. 3,

$$\text{Porosity} = (1 - R) \times 100. \tag{3}$$

2.5 Mechanical properties analysis

In the assessment of the mechanical properties of the produced composites, a tensile test was conducted in accordance with ASTM E 8 (ASTM E 8, 2022). A weight of 100 kN at a

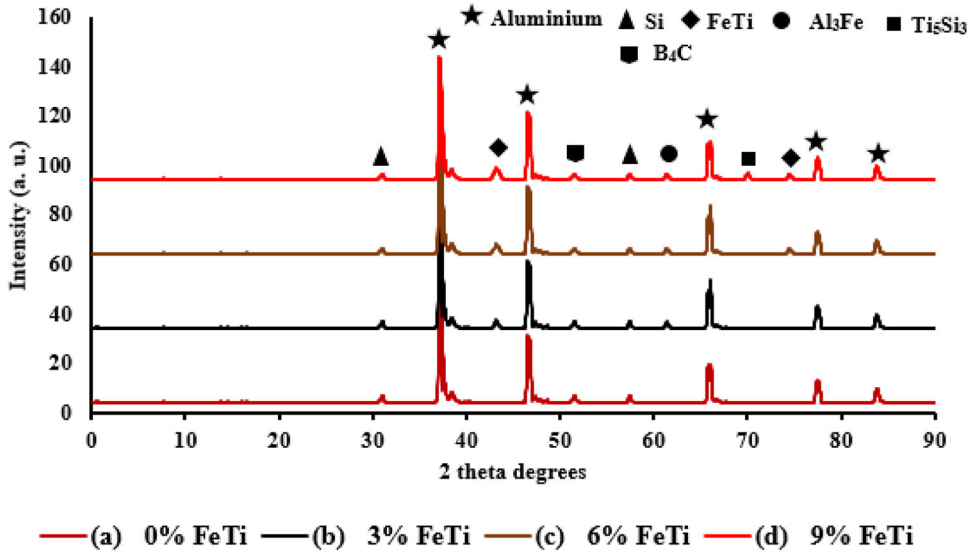

Fig. 2 XRD diffraction patterns for the Al-12Si/B_4C/FeTi composite

strain rate of 2×10^{-3}/s was applied to the specimens measuring 120 mm in length with a gauge length of 30 mm and a 10 mm gauge diameter. A hardness test was performed using the ASTM E384 (2022) standard, and a microhardness tester (MHT-1000 T) was employed to measure the Vickers hardness.

3 Results and discussion

3.1 Microstructural characterization

3.1.1 X-ray diffraction analysis of the composites

Figure 2 shows the diffraction pattern and the evolution of the present phases in the developed composites. It was observed that the major peaks present in the reference composite (Al-12Si/5B_4C) were mostly alpha-aluminum, silicon, and B_4C peaks attributed to the constituent phases inherent in the reference composite (Al-12Si/5B_4C). The inclusion of the FeTi particle at 3 wt.% triggered the existence of a secondary FeTi phase at 3% FeTi addition (Fig. 3b). These peaks were noted to increase in intensities at 6 and 9 wt.% FeTi addition (Fig. 3c and Fig. 3d). Furthermore, peaks of eutectic iron (Al_3Fe) were identified upon inclusion of FeTi particles at 3, 6, and 9 wt.%. At 9% FeTi, a titanium silicide (Ti_5Si_3) phase was also observed.

3.1.2 Microstructural Analysis of the composites produced

The SEM images of the produced composites are shown in Fig. 3a–d. White spots (labeled spot "1") were identified in Fig. 3a. From the elemental results (Fig. 4d), it was determined that these spots are mostly composed of boron and carbon, typical of boron carbide. This indicates that at 0% FeTi, the matrix primarily contained dispersed B4C particles, along with the occurrence of pores alongside the B4C particles. In Fig. 3b–d, dark spots were also observed to be dispersed within the composite matrixes. Elemental analysis revealed that the dark spots labeled "spot 2" predominantly consisted of titanium and iron, characteristic of ferrotitanium (FeTi) (Fig. 4a). Therefore, FeTi particles were detected within the matrix at 3, 6, and 9% FeTi addition. Additionally, white threads along the grain boundary, labeled "3," were observed. Elemental composition analysis indicated that these white threads were predominantly composed of aluminum and iron (Fig. 4b), consistent with the elemental composition of eutectic iron (Al3Fe) in the aluminum matrix (Elsharkawi et al. 2022; Shakiba et al. 2014).

The spots initially identified as 1, 2, and 3 were also found in Fig. 3d at 9% FeTi, accompanied by the presence of an intermetallic titanium silicide (Ti5Si3) phase, labeled as spot "4." The elemental composition analysis depicted in Fig. 4c confirmed the presence of the titanium silicide phase, aligning with findings by Pribytkov et al. (2022). All these characteristics support the identification of phases whose peaks were observed in the X-ray diffraction analysis (Fig. 2).

3.2 Physical properties analysis

3.2.1 Porosity

Figure 5 illustrates the porosity of the composites with respect to the rise in FeTi proportion within the matrix. It was observed that the porosity value decreased as the weight percentage of FeTi increased. As compared with reference mix, 3%, 6%, and 9% dosage of FeTi experienced a percentage decrease of 3.70, 6.79, and 8.64%, respectively (Fig. 5).

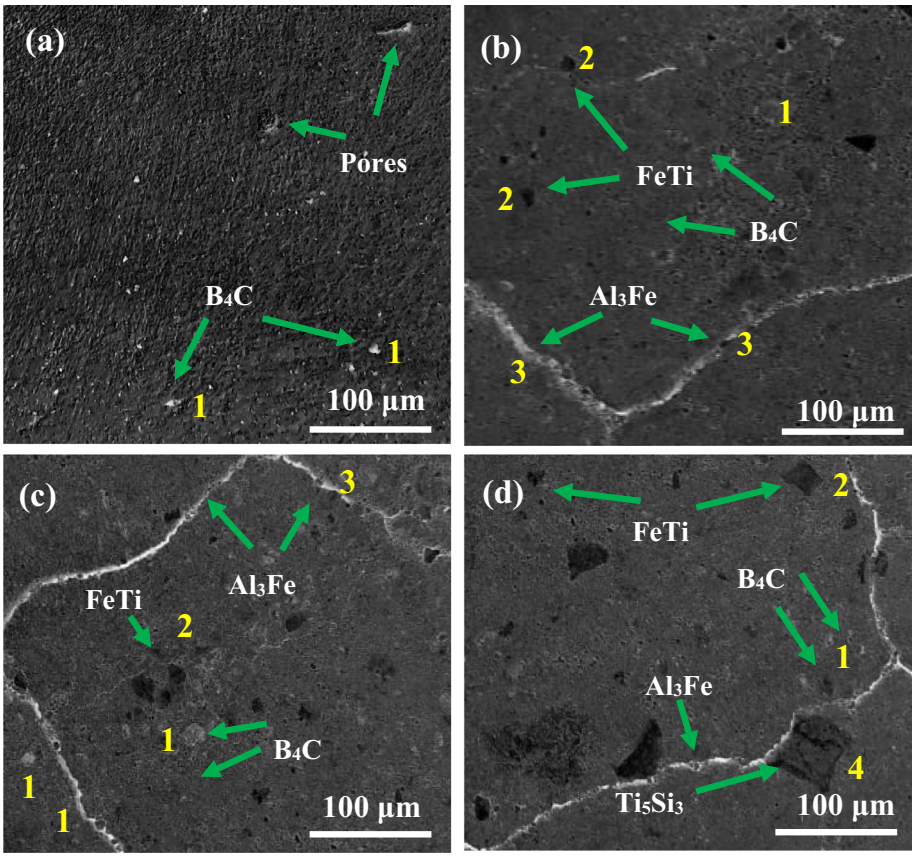

Fig. 3 Microstructural features of the sintered composites **a** 0% FeTi **b** 3% FeTi **c** 6% FeTi **d** 9% FeTi

The porosity observed at 0% FeTi is linked to solidification shrinkage and gas segregation, as indicated by Dehgahi et al. (2020). With the inclusion of FeTi in increasing proportion, porosity begins to decrease. This can be attributed to the ability of FeTi particles to fill existing pores and voids, consistent with the findings of Akinwande et al. (2023a, b, c), and Olaniran et al. (2022a, b), who observed a progressive decline in porosity with increasing particle fillers.

3.2.2 Density and relative density examination

The graph illustrating the density and relative density of the composites as a function of FeTi dosage in wt.% is shown in Fig. 6. The density of the matrix is 2.73 g/cc, while the density of B_4C is 2.53 g/cm^3, and the density of FeTi is 3.0 g/cm^3. It was observed that the addition of FeTi led to a linear increase in the relative density and density of the composites. Introduction of 3, 6, and 9 wt% of FeTi into the reference composite increases its density by 2.2, 3.6, and 4.7%, respectively, and its relative density by 0.7, 1.1, and 1.4%, respectively. This is partly due to the fact that density of FeTi is higher than that of the matrix and B_4C. As further observed, the relative density enhancement is a result of the porosity decrement as the dosage of FeTi increases in the composite. Furthermore, Olaniran et al. (2022a, b) revealed that the addition of molybdenum particles to the sintering process resulted in a rise in the density of aluminum alloy in a similar manner to that reported in this work. Shirvanimoghaddam et al. (2015) also discovered that adding particles as fillers to an aluminum matrix enhanced the composite's density.

3.3 Mechanical properties of the fabricated composites

The mechanical characteristics of the produced composites, such as their tensile strength, ultimate strength, yield strength, elongation, and hardness, are covered in this section.

3.3.1 Tensile performance

Figure 7 shows the relationship between the tensile load and tensile strain of the composite materials. It was depicted that the yield strength of the composites increases as the percentage weight of FeTi increases. Furthermore, it was observed that the ductility of the composites produced decreased with an increase in the proportion of FeTi reinforcement. More information about the ultimate strength, yield strength, elongation, and hardness is illustrated in Figs. 8 and 9.

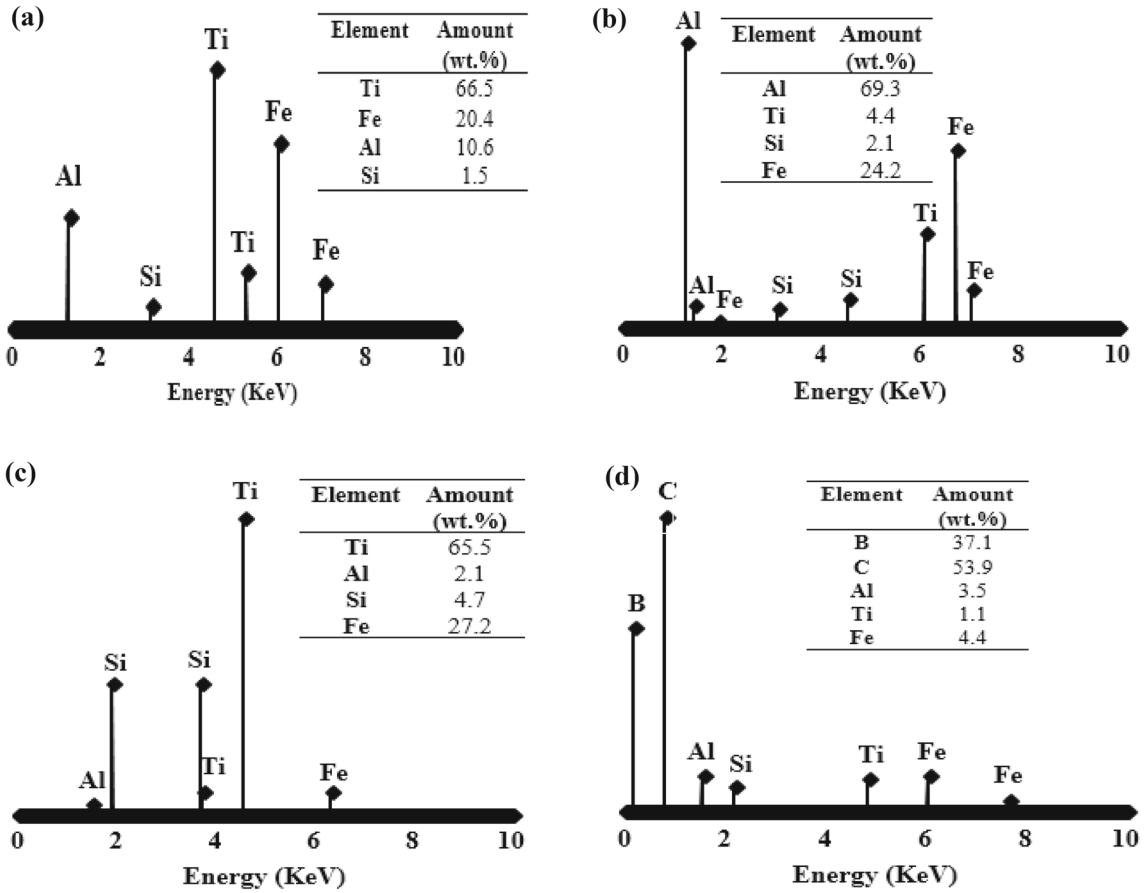

Fig. 4 Elemental composition as analyzed by EDX for the phases **a** FeTi **b** Al_3Fe **c** Ti_5Si_3 **d** B_4C present in the composite as revealed by XRD analysis

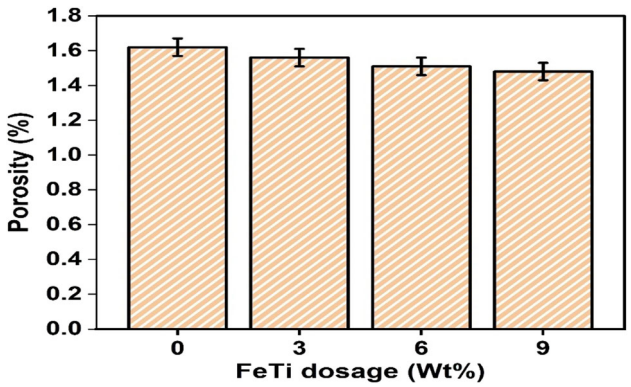

Fig. 5 Porosity variation in the produced composites

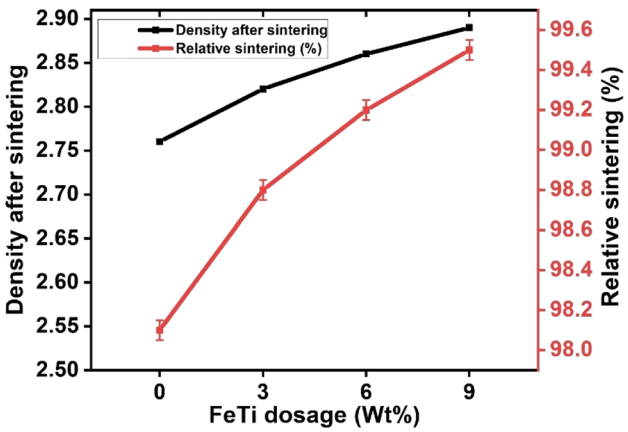

Fig. 6 Variation in density and relative density as function of FeTi %

3.3.2 Yield and ultimate strength

As shown in Fig. 8, it was observed that the yield strength of the fabricated composites increased as the amount of FeTi increased at 3, 6, and 9 wt% by 11.8, 19.7, and 25%, respectively, as compared to the reference composite. The significant increase in the yield strength of the composites with the inclusion of FeTi is partly as a result of the particle dispersion within the matrix, which played a role in the pinning of dislocation during deformation (Zhang et al. 2022; Ananiadis et al. 2022).

Equally, the Al_3Fe appearing at the grain boundary contributed to the inhibition of dislocation movement, eventually

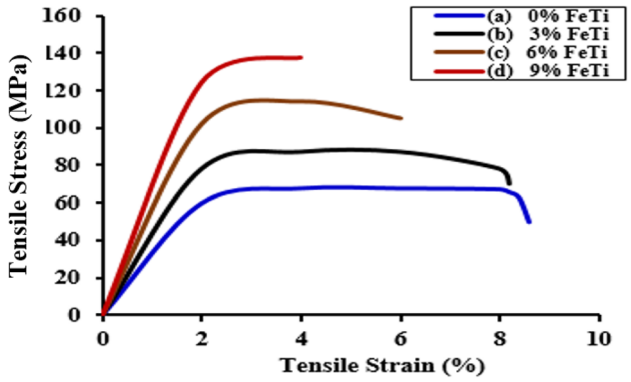

Fig. 7 Tensile stress–strain characteristics of the developed Al-12%Si/5%B_4C/FeTi composite

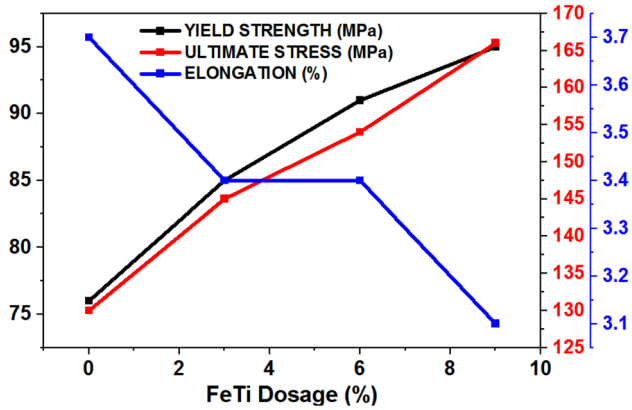

Fig. 8 Graph showing the strength and elongation behavior of the produced composites

resulting in the improvement of the strength of the composite (Dangwal et al. 2023; Javaid et al. 2021). Consequently, the higher the FeTi weight percentage, the higher the yield strength; this is evident in the composite, with 9 wt.% of FeTi exhibiting an improvement in yield strength of 25% relative to the reference composite. Similarly, for ultimate strength performance, a percentage rise in FeTi proportion led to an increase in ultimate strength. Again, in this case, composites with a 9% percentage weight of FeTi possess the highest ultimate strength of 27.7%.

Both the yield strength and the ultimate strength of the composites appreciated in value because of the dispersion of the reinforcing particles. This is clear from the SEM image (Fig. 3). The dispersion of particles within the matrix facilitated interaction between the matrix and reinforcement, leading to a homogeneous stress distribution. Additionally, the presence of these particles hindered dislocation movement in the matrix, resulting in more dislocations forming around the particles. This increase in dislocation density contributed to the enhancement of the composite's strength. These findings align with a study by Yigezy et al. (2013),

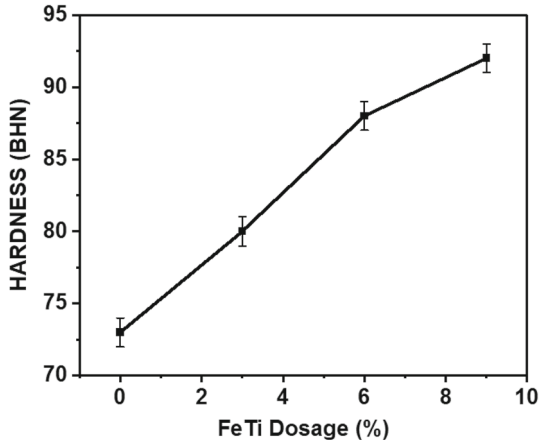

Fig. 9 Hardness performance of the produced composites

which also observed improved strength performance in aluminum composites upon the inclusion of reinforcing particles in increasing proportions.

3.3.3 Elongation

Figure 8 depicts a linear decrement in elongation as the amount of FeTi increases in the aluminum alloy/B_4C composites. This is so based on the improvement of the stiffness of the composites resulting from the inclusion of the reinforcing phase. This result further affirmed the outcome of Wu et al. 2022, in which the progressive presence of TiB_2 at 1, 2, 3, 4, and 5% in aluminum A356 within the matrix. Similarly, the results reported in this study regarding elongation corroborate the findings of Rajesh et al. (2023), and Raksha et al. (2023).

3.3.4 Hardness

Figure 9 presents the hardness plot of the composites produced. It was observed that the hardness increased with the rise in FeTi dosage, which could be attributed to the inherent hardness property of FeTi, as reported by Chu et al. (2020). The SEM image in Fig. 3 revealed finer grains and greater particle cohesiveness, which might also contribute to the increased hardness, as noted in studies by Kumar et al. (2023a, b, c) and Huan et al. (2022). These findings are consistent with the work of Yilmaz et al. (2022), who reported enhanced hardness in Cu matrix reinforced with varying proportions of FeTi (6, 9, 12, 15, and 18%). Similarly, Ravichandran et al. (2021) demonstrated improved hardness in aluminum alloy (AA7075) when infused with molybdenum disulfide and aluminum nitride in increasing proportions. The hardness value was found to be highest

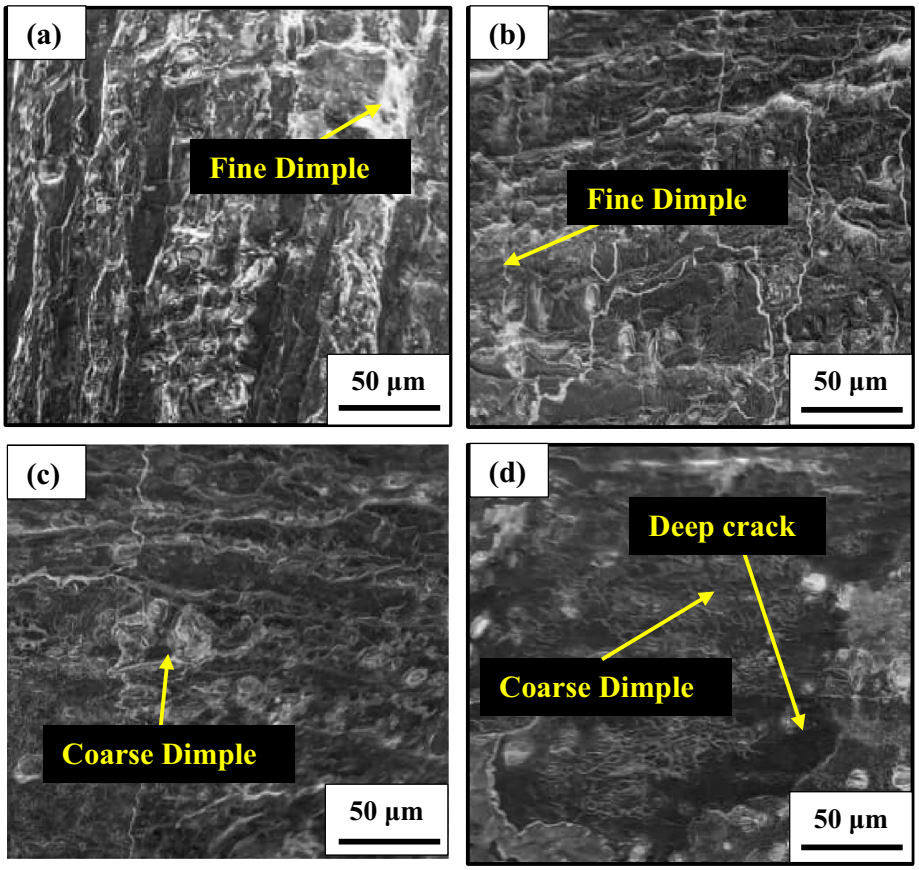

Fig. 10 Tensile fractography of the developed composites at **a** 0% FeTi **b** 3% FeTi **c** 6% FeTi **d** 9% FeTi

when 9% FeTi was incorporated, attributable to the mechanisms discussed earlier and the presence of the hard Ti5Si3 phase (Fig. 3d).

3.4 Tensile fractographic examination

The micrograph in Fig. 10 shows the tensile fractography of Al-12%Si/5%B_4C/FeTi composites. The tensile fractography of reference at 0 wt.% FeTi is shown in Fig. 10a, and the most noticeable features are fine dimples associated with relatively ductile fracture. According to Fig. 10b–d, the reduced ductility of the materials with a rising percentage of FeTi led to a reduction in the fine dimple fracture of the composites. The fractography also reveals a smooth fracture surface with worn tracks and tear ridges. Maleque et al. (2017) claimed that fracture in composite materials occurs as a result of crack initiation that occurs immediately at the boundary between the aluminum alloy and reinforcement.

The ductile properties are demonstrated by the wear tracks and tear ridges visible on the fracture surface. Additionally, as shown in Fig. 10b, c, FeTi and B_4C particles could be visible on the surface of the shattered specimen, providing proof of appropriate bonding between the reinforcements and matrix. The proper settling of FeTi particles with the grain of the aluminum-boron carbide matrix, which led to a reduction in shear deformation in the tensile direction, may be responsible for the decrease in dimples generated on the surface of the sample with the highest reinforcement. The FeTi particles and the coarse intermetallic that formed in the composites may be the cause of the cracks shown in Fig. 10d.

4 Conclusion

In summary, the outcomes of this study offer valuable insights into the mechanical enhancement of Al-12% Si through the incorporation of FeTi particles. The observed phases, including B4C, FeTi, AlFe3, and the identification of intermetallic Ti5Fe3 at 9% FeTi, contribute to our understanding of the composite's microstructure. SEM micrographs confirm the effective dispersion of B4C and FeTi within the composites. A noticeable decrease in porosity, coupled with a significant increase in density and relative density, demonstrates the positive impact of FeTi on the physical properties of the composites. Furthermore, the systematic improvement in yield strength, ultimate strength, and hardness with increasing FeTi content highlights the effectiveness of FeTi as a reinforcing agent. However, the linear reduction in elongation suggests a trade-off between strength and ductility. The

fractographic analysis reveals a transition from fine dimples to coarser dimples, indicating the evolving fracture behavior with higher FeTi dosage. While these findings contribute to the understanding of hybridized Al-12% Si composites, further research may be warranted to explore specific applications and optimize the balance between strength and ductility.

Author contributions OTO and AAA contributed to conceptualization, data curation, methodology, literature review manuscript drafting, and editing; OSA and OOS were involved in data curation, methodology, literature review, manuscript drafting, and editing; BAO performed project management and administration, and supervision.

Funding The work received no funding from any organization.

Data availability Data shall be made available by the authors on request.

Declarations

Competing interests The authors declare no competing interests.

Conflict of interest The authors declare no competing interest that may affect the publication and readability of the paper.

References

Adediran AA, Akinwande AA, Balogun OA, Adesina OS, Olayanju A, Mojisola T (2021) Evaluation of the properties of Al-6061 alloy reinforced with particulate waste glass. Sci Afri 12(2021):e00812

Adediran AA, Akinwande AA, Adesina OS, Agboso V, Balogun OA, Kumar BR (2023) Modeling and optimization of green-Al 6061 prepared from environmentally sourced materials. Heliyon 9:e18474. https://doi.org/10.1016/j.heliyon.2023.e18474

Akinwamide SO, Lemika SM, Obadele BA, Akinribide OJ, Falodun OE, Olumbambi PA, Abe BT (2019a) A nanoindentation study on Al(TiFe-Mg-SiC) composites fabricated by stir casting. Key Eng Mater 821:81–88. https://doi.org/10.4028/www.scientific.net/KEM.821.81

Akinwamide SO, Lemika SM, Obadele AO, Akinribide O, Abe BT, Olubambi PA (2019b) Characterization and mechanical response of novel Al-(Mg-TiFe-SiC) metal matrix composites developed by stir casting technique. J Compos Mater. https://doi.org/10.1177/0021998319851198

Akinwamide SO, Abe BT, Akinribide OJ, Obadele BA, Olubambi PA (2020) Characterization of microstructure, mechanical properties and corrosion response of aluminium-based composites fabricated via casting-a review. Int J Adv Manuf Technol 109:975–991. https://doi.org/10.1007/s00170-020-05703-1

Akinwamide SO, Akinribide OJ, Olubambi PA (2021) Influence of ferrotitanium and silicon carbide addition on structural modification, nanohardness and corrosion behaviour of stir-cast aluminium matrix composites. SILICON 13:2221–2232. https://doi.org/10.1007/s12633-020-00733-6

Akinwande AA, Kumar MS, Adesina OS, Adediran AA, Romanovski V, Salah B (2023a) Tribological performance of a novel 7068-aluminium/lightweight-high-entropy-alloy fabricated via powder metallurgy. Mater Chem Phys 308:128207. https://doi.org/10.1016/j.matchemphys.2023.128207

Akinwande AA, Moskovskikh D, Romanovskaia E, Kumar JP, Romanovski V (2023b) Applicability of extreme vertices design in the compositional optimization of 3D-printed lightweight high-entropy-alloy/B4C/ZrO2 titanium trihybrid aero-composite. Math Comput Appl 28:54. https://doi.org/10.3390/mca28020054

Akinwande AA, Adesina OS, Adediran AA, Balogun OA, Mukuro D, Balogun OP, Kumar MS (2023c) Microstructure, process optimization, and strength response modelling of green-aluminium-6061 composite as automobile material. Ceramics 6(1):386–415

Alshmri F (2013) Lightweight material: aluminium high silicon alloys in the automotive industry. Adv Mater Res 774–776:1271–1276. https://doi.org/10.4028/www.scientific.net/AMR.774-776.1271

Ananiadis EA, Karantzalis AE, Exarchos DA, Matikas TE (2022) Al-RHEA particulates MMCs by PM route: mechanical properties and sliding wear response. Appl Mech 3(3):1145–1162. https://doi.org/10.3390/applmech3030065

ASTM E 8 (2022) Standard test methods for tension testing of metallic materials. ASTM International. https://doi.org/10.1520/E0008_E0008M-22

ASTM E384 (2022) Standard test methods for microindentation hardness of materials. ASTM International. https://doi.org/10.1520/E0384-17

Balogun OA, Akinwande AA, Adediran AA, Ogunsanya OA, Ademati AO, Kumar MS, Akinlabi ET (2022) Microstructure and particle size effects on selected mechanical properties of waste glass-reinforced aluminium matrix composites. Mater Today Proc 62:4589–4598

Bolat Ç, Akgün İC, Gökşenli A (2021) Effects of particle size, bimodality and heat treatment on mechanical properties of pumice reinforced aluminum syntactic foams produced by cold chamber die casting. China Found 18(6):529–540. https://doi.org/10.1007/s41230-021-1133-4

Bolat Ç, Akgün İC, Gökşenli A (2022) Influences of reinforcement size and artificial aging on the compression features of hybrid ceramic filled aluminum syntactic foams. Proc Inst Mech Eng C J Mech Eng Sci 236(14):8027–8037. https://doi.org/10.1177/09544062221083208

Chandel R, Sharma N, Bansal SA (2021) A review on recent developments of aluminum-based hybrid composites for automotive applications. Emergent Mater 4(5):1243–1257. https://doi.org/10.1007/s42247-021-00186-6

Chu Q, Tong X, Xu S, Zhang M, Li J, Yan F, Yan C (2020) Interfacial investigation of explosion-welded titanium/steel bimetallic plates. J Mater Eng Perform 29:78–86

Dangwal S, Edalati K, Valiev RZ, Langdon TG (2023) Breaks in the Hall-Petch relationship after severe plastic deformation of magnesium, aluminium, copper, and iron. Crystals. https://doi.org/10.3390/cryst13030413

Das DK, Mishra PC, Singh S, Pattanaik S (2014) Fabrication and heat treatment of ceramic-reinforced aluminium matrix composites-a review. Int J Mech Mater Eng 9:1–15

Dehgahi S, Ghoncheh MH, Hadadzadeh A, Sanjari M, Amirkhiz BS, Mohammadi M (2020) The role of titanium on the microstructure and mechanical properties of additively manufactured C300 maraging steels. Mater Des 194:108965

Dursun T, Soutis C (2014) Recent developments in advanced aircraft aluminium alloys. Mater Des 1980–2015(56):862–871

Elsharkawi EA, MacNeil D, Chen XG (2022) Exploring the effect of Ni as an impurity on Fe-rich phases in simulated direct chill casting Al-Fe-Si alloys. Metallogr Microstr Anal 11:724–735. https://doi.org/10.1007/s13632-022-00894-3

Haber D (2015) Lightweight materials for automotive applications: a review. SAE Technical Paper 2015–36–0219, 2015, https://doi.org/10.4271/2015-36-0219.

Halil K, İsmail O, Sibel D, Ramazan Ç (2019) Wear and mechanical properties of Al6061/SiC/B4C hybrid composites produced with powder metallurgy. J Market Res 8(6):5348–5361. https://doi.org/10.1016/j.jmrt.2019.09.002

Han S, Guang X, Li Z, Li Y (2022) Joining processes of CFRP-Al sheets in automobile lightweighting technologies: A review. Polym Compos 43(12):8622–8633

Huan C, He Y, Su Q, Zuo L, Ren C, Xu H, Liu Y (2022) Properties of AlFeNiCrCoTi0.5 high-entropy alloy particle-reinforced 6061Al composites prepared by extrusion. Metals 12(8):1325

Javaid F, Pouriayevali H, Durst K (2021) Dislocation-grain boundary interactions: recent advances on the underlying mechanisms studied via nanoindentation testing. J Mater Res 36(12):2545–2557. https://doi.org/10.1557/s43578-020-00096-z

Joost WJ, Krajewski PE (2017) Towards magnesium alloys for high-volume automotive applications. Scripta Mater 128:107–112

Khademian N, Peimaei Y (2020) Lightweight materials (LWM) in transportation especially application of aluminum in light weight automobiles (LWA). In: International Conference on interdisciplinary studies in nanotechnology, pp 1–22

Khan et al (2020) Effect of mixing method and particle size on hardness an compressive strength of aluminium based metal matrix composite prepared through powder metallurgy route. J Mater Res 18:282–292. https://doi.org/10.1016/j.jmrt.2022.02.094. (**Sankhla A M., Patel K M., Makhesana M A., Giasin K., Pimenov D Y., Wojciechowski S., Khanna N., 2022.**)

Kumar JP, Smart R, Manova S, Akinwande AA, Kumar MS (2023a) Mechanical and tribological assessment of AA7075 reinforced Si_3N_4/TaC/Ti hybrid metal matrix composites processed through stir casting process. Adv Mater Process Technol. https://doi.org/10.1080/2374068X.2023.2215603

Kumar MS, Akinwande AA, Yang CH, Margabandu V, Romanovski V (2023b) Investigation on mechanical behavior of Al-Mg-Si alloy hybridized with calcined eggshell and TiO_2 particulates. Biomass Convers Biorefin. https://doi.org/10.1007/s13399-023-04215-8

Kumar MS, Akinwande AA, Yang CH, Vignesh M, Romanovski V (2023c) Investigation on mechanical behaviour of Al–Mg-Si alloy hybridized with calcined eggshell and TiO2 particulates. Biomass Convers Biorefin. https://doi.org/10.1007/s13399-023-04215-8

Maleque MA, Adebisi AA, Izzati N (2017) Analysis of fracture mechanism for Al-Mg/SiCp composite materials. IOP Conf Ser Mater Sci Eng 184(1):012031

Mazahery A, Ostad Shabani M (2012) Mechanical Properties of Squeeze-Cast A356 Composites Reinforced With B4C Particulates. J Mater Eng Perform 21(2):247–252. https://doi.org/10.1007/s11665-011-9867-6

Mazahery A, Shabani MO, Salahi E, Rahimipour MR, Tofigh AA, Razavi M (2012) Hardness and tensile strength study on Al356–B 4 C composites. Mater Sci Technol 28(5):634–638. https://doi.org/10.1179/1743284710Y.0000000010

Musfirah AH, Jaharah AG (2012) Magnesium and aluminum alloys in automotive industry. J Appl Sci Res 8(9):4865–4875

Ogunbiyi O, Tian Y, Akinwande AA, Rominiyi AL (2023) AA7075/HEA composites fabricated by microwave sintering: assessment of the microstructural features and response surface optimization. Intermetallics 155:107830. https://doi.org/10.1016/j.intermet.2023.107830

Ogunsanya OA, Akinwande AA, Balogun OA, Romanovski V, Kumar MS (2022) Mechanical and damping behavior of artificially aged Al 6061/TiO2 reinforced composites for aerospace applications. Part Sci Technol. https://doi.org/10.1080/02726351.2022.2065652

Ogunsanya OA, Akinwande AA, Radhakrishnan RM, Talabi HK, Kumar MS, Margabandu V, Bhowmik A (2023) Investigation on mechanical behavior of Al-Mg-Si alloy hybridized with calcined eggshell and TiO_2 particulates. Biomass Conv Bioref. https://doi.org/10.1007/s13399-023-04215-8

Olaniran O, Akinwande AA, Adediran AA, Jen TC (2022a) Microstructural characterization and properties of aluminium 7075/Mo prepared by microwave sintering for high-strength application. Adv Mater Process Technol. https://doi.org/10.1080/2374068X.2022.2130894

Olaniran O, Akinwande AA, Adediran AA, Jen TC (2022b) Process maps and regression models for the physio-thermo-mechanical properties of sintered Al7075-molybdenum composite. Mater Lett. https://doi.org/10.1016/j.matlet.2022.133527

Olaniran O, Akinwande AA, Adediran AA, Jen TC (2023) Process maps and regression models for the physio-thermo-mechanical properties of sintered Al7075-molybdenum composite. Mater Lett 332:133527. https://doi.org/10.1016/j.matlet.2022.133527

Olorunyolemi OC, Ogunsanya OA, Akinwande AA, Balogun OA, Kumar MS (2022) Enhanced mechanical behavior and grain characteristics of aluminium matrix composites by cold rolling and reinforcement addition (rice husk ash and coal fly ash). J Process Mech Eng. https://doi.org/10.1177/09544089221124462

Orłowicz AW, Mróz M, Tupaj M, Trytek A (2015) Materials used in the automotive industry. Arch Found Engg 15:75–78

Parikh VK, Patel V, Pandya DP, Andersson J (2023) Current status on manufacturing routes to produce metal matrix composites: state-of-the-art. Heliyon. 9(2):e13558. https://doi.org/10.1016/j.heliyon.2023.e13558

Patel M, Pardhi B, Chopara S, Pal M (2018) Lightweight composite materials for automotive-a review. Carbon 1(2500):151

Pribytkov GA, Krinitsyn MG, Korzhova VV, Firsina IA, Korosteleva EN (2022) Structure and oxidation resistance of titanium silicide Ti_5Si_3-titanium binder powder composites. Protection of Metals and Physical Chemistry 58:70–75. https://doi.org/10.1134/S2070205122010016

Rajesh RM, Kumar KD, Sailender M, Prasad GP, Nagaraj N, Ramulu PJ (2023) Effect of boron carbide particles addition on the mechanical and wear behavior of aluminium alloy composites. Adv Mater Sci Eng 2023:1–10. https://doi.org/10.1155/2023/2386558

Raksha MS, Adaveesh B, Nagaral M, Boppana SB, Anjinappa C, Khan MS, Wahab MOA, Islam S, Bhardwaj V, Palavalasa RK, Khan MA, Razak A (2023) Impact of boron carbide particles mand weight percentage on the mechanical and wear characterization of Al2011 alloy metal composites. ACS Omega 8:23763–23771. https://doi.org/10.1021/acsomega.3c02065

Ramadoss N, Pazhanivel K, Anbuchezhiyan G (2020) Synthesis of B4C and BN reinforced Al7075 hybrid composites using stir casting method. J Mater Res 9(3):6297–6304. https://doi.org/10.1016/j.jmrt.2020.03.043

Ravichandran M, Mohanavel V, Sathish T, Ganeshan P, Kumar SS, Subbiah R (2021) Mechanical properties of AlN and molybdenum disulfide reinforced aluminium alloy matrix composites. J Phys Conf Ser 2027(1):012010

Sahu S, Ansari MZ, Mondal DP (2020) Microstructure and compressive deformation behavior of 2014 aluminium cenosphere syntactic foam made through stircasting technique. Mater Today Proc 25:785–788. https://doi.org/10.1016/j.matpr.2019.09.019

Sankhla AM, Patel KM, Makhesana MA, Giasin K, Pimenov DY, Wojciechowski S, Khanna N (2022) Effect of mixing method and particle size on hardness an compressive strength of aluminium based metal matrix composite prepared through powder metallurgy route. J Mater Res 18:282–292. https://doi.org/10.1016/j.jmrt.2022.02.094

Satyanarayana T, Rao PS, Krishna MG (2019) Influence of wear parameters on friction performance of A356 aluminum—graphite/ granite particles reinforced metal matrix hybrid composites. Heliyon 5(6):e01770. https://doi.org/10.1016/j.heliyon.2019.e01770

Shakiba M, Parson N, Chen XG (2014) Effect of homogenization treatment and silicon content on the microstructure and hot workability of dilute Al-Fe-Si. Mater Sci Eng A 619:180–189. https://doi.org/10.1016/j.msea.2014.09.072

Sharma DK, Sharma M, Upadhyay G (2019) Boron carbide (B4C) reinforced aluminum matrix composites (AMCs). Int J Innov Technol Explor Eng 9(1):2194

Sharma AK, Bhandari R, Aherwar A, Rimašauskienė R (2020) Matrix materials used in composites: a comprehensive study. Mater Today Proc 21:1559–1562. https://doi.org/10.1016/j.matpr.2019.11.086

Sharma SK, Saxena KK, Kumar N (2022) Effect of SiC on mechanical properties of Al-based metal matrix composites produced by stir casting. Met Sci Heat Treat 64:316–320. https://doi.org/10.1007/s11041-022-00807-9

Shirvanimoghaddam K, Khayyam H, Abdizadeh H, Akbari MK, Pakseresht AH, Abdi F, Abbasi A, Naebe M (2015) Effect of B4C, TiB2 and ZrSiO4 ceramic particles on mechanical properties of aluminium matrix composites: experimental investigation and predictive modeling. Ceram Int. https://doi.org/10.1016/j.ceramint.2015.12.181

Wu W, Zeng T, Hao W, Jiang S (2022) Microstructure and mechanical properties of aluminium matrix composites reinforced with in-situ TiB2 particles. Front Mate 9:1–9. https://doi.org/10.3389/fmats.2022.817376

Xu G, Yu Y, Zhang Y, Li T, Wang T (2019) Effect of B4C particle size on the mechanical properties of B4C reinforced aluminum matrix layered composite. Sci Eng Compos Mater 26(1):53–61. https://doi.org/10.1515/secm-2018-0072

Yigezy et al (2013) Processing and characterization of advanced lightweight composites for engineering applications. Adv Mater Sci Eng 2022:1–7. https://doi.org/10.1155/2022/2381425. (**Periasamy K., Ganesh S., Kumar S C., M. Nandhakumar S., Thirugnanasambandham T., Gurmesa M. D., 2022.**)

Yilmaz SO, Teker T, Karabeyoğlu SS (2022) Metallographic study and wear behavior of Cu-BASED FeTi-REINFORCED composites. Surf Rev Lett 29(04):2250043. https://doi.org/10.1142/s0218625x22500433

Zhang X, Lu W, Chen T (2022) Multiscale and dual-structured reinforced particulates enhance the strength of aluminium matrix composites at no ductility loss. Mater Sci Eng, A 856:144003. https://doi.org/10.1016/j.msea.2022.144003

Zheng K, Politis DJ, Wang L, Lin J (2018) A review on forming techniques for manufacturing lightweight complex—shaped aluminium panel components. Int J Lightweight Mater Manuf 1(2):55–80. https://doi.org/10.1016/j.ijlmm.2018.03.006